The Performance of Chip-Scale Atomic Clocks

S. Knappe, P. Schwindt, L. Hollberg, and J. Kitching
Time and Frequency Division, National Institute of Standards and Technology, 325 Broadway, Boulder CO 80305
phone: (303) 497 3334, fax:(303) 497 7845, knappe@boulder.nist.gov
V. Shah
also with: Department of Physics, University of Colorado, Boulder, CO, 80309
V. Gerginov
also with: Department of Physics, University of Notre Dame, Notre Dame, IN 45665

Abstract: We compare the performance of two chip-scale atomic clock physics packages, one based on excitation using the D_2 line of Cs and the other using the D_1 line of ^{87}Rb.
©2005 Optical Society of America
OCIS codes: (300.6320) Spectroscopy, high-resolution; (350.3950) Micro-optics

We compare the performance of two chip-scale atomic clock physics packages [1] in terms of frequency stability and power consumption. This recently developed chip-scale clock technology is based on coherent-population-trapping (CPT) excitation of hyperfine transitions in thermal vapors of alkali atoms confined in microfabricated cells. The two physics packages differ in that one is based on Cs, excited on the D_2 transition, while the other is based on ^{87}Rb excited on the D_1 transition. We find that while the ^{87}Rb-D1 device achieved superior short-term frequency stability than the Cs-D2 device, its power consumption was higher due to the higher operating temperature of the vapor cell. Chip-scale atomic clocks (CSACs) and magnetometers [2] promise to bring high-precision timing and high-sensitivity sensing to a variety of portable, battery-operated applications [3,4].

The chip-scale clocks being developed at NIST are passive, vapor-cell frequency references in which a microwave oscillator is stabilized to a CPT resonance excited in a vapor of alkali atoms. The current of a vertical-cavity surface-emitting laser (VCSEL) is modulated at a frequency that is half the ground state hyperfine splitting of the alkali atoms. The laser wavelength is tuned so that the two first-order modulation sidebands, containing roughly 60 % of the optical power, are in resonance with the transitions from the two ground-state hyperfine components to the excited state, forming a so-called Λ-system. When the modulation frequency is tuned so that its second harmonic is equal to the hyperfine splitting, a ground-state coherence can be induced, out of phase with the driving light fields [5]. This gives rise to a narrow bright line in the transmission spectrum,. Suitable transitions for the CPT spectroscopy are the D_1 and D_2 lines of Cs and ^{87}Rb, since these atoms have relatively large ground-state hyperfine splittings and since VCSELs at the optical wavelengths corresponding to these transitions are commercially available.

Both physics packages tested have a volume of about 10 mm^3 and are designed in a similar way [1] as shown in Fig. 1.At the base of the clock a VCSEL is mounted onto a baseplate. The light emitted from the laser is collimated, attenuated, and circularly polarized by a micro-optics assembly, mounted above the laser. The light is then sent through a microfabricated atomic vapor cell [6,7], assembled with integrated heaters, and the transmitted power is detected with a photodiode, mounted at the top of the stack. A longitudinal magnetic field is applied to split the Zeeman levels apart and a magnetic shield reduces external stray fields. As the laser modulation frequency is scanned near one-half the hyperfine transition frequency, a number of resonances can be seen in transmission: 3 for ^{87}Rb and 7 for Cs (see Fig. 2). These resonances are generated by the coupling of two Zeeman states with the same magnetic quantum numbers, one from each hyperfine component. The center resonance is the one probed for the clock, since it is only sensitive to magnetic fields in second order. The other resonances can be used for a sensitive chip-scale magnetometer.

Photodiode

Alkali-Vapor Cell

Micro-Optics Assembly

VCSEL
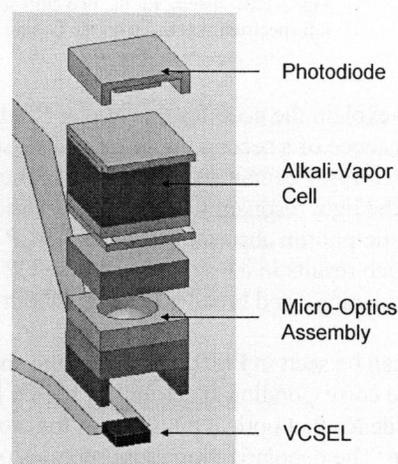
Fig. 1. Setup of the chip-scale atomic clocks physics package.

Both clocks operate at a similar laser intensity of about 20 mW/cm^2, both cells were heated to a temperature where roughly 25 % of the light was absorbed and both contained a buffer gas at a similar pressure, about 32 kPa. It can be seen from Fig. 2 that the amplitude of the center resonance, normalized to the background absorption, is significantly higher for the Rb D$_1$ line than for the Cs D$_2$ line. One reason for this improvement is that ^{87}Rb only has half the number of ground state Zeeman components compared to Cs. In addition, the Cs-D$_2$ line has a more complicated excited state hyperfine structure, including states that couple to one ground state only [8,9]. Both of these effects reduce the number of atoms in the coherent trapped state and thus, the resonance contrast.

In addition, the lifetime of the ground-state coherence is reduced by single-photon transitions to these detrimental excited states on the D$_2$ line. As a result, the broadening of the resonances with optical power is larger on the D$_2$ transition, as compared with the D$_1$ transition. In fact, more than half of the CPT linewidth of 7.1 kHz of the Cs D$_2$ CSAC is caused by power broadening. The remaining width can be attributed to wall collisions, with minor contributions from buffer gas and spin-exchange collisions. In contrast, for the ^{87}Rb D$_1$ line, we believe that spin-exchange collisions cause most of the broadening and that power broadening contributes to only 40 % of the CPT linewidth. The increased importance of spin-exchange broadening occurs because the Rb cell has to be heated to 120 °C in order to achieve the same optical absorption as the Cs cell operating at 85 °C. The temperature of the Rb cell corresponds to a vapor pressure of Rb more than twice the value expected in order to achieve 25 % absorption, while for the Cs device, the cell temperature of 85 °C agrees with the expected vapor pressure for 25 % absorption.
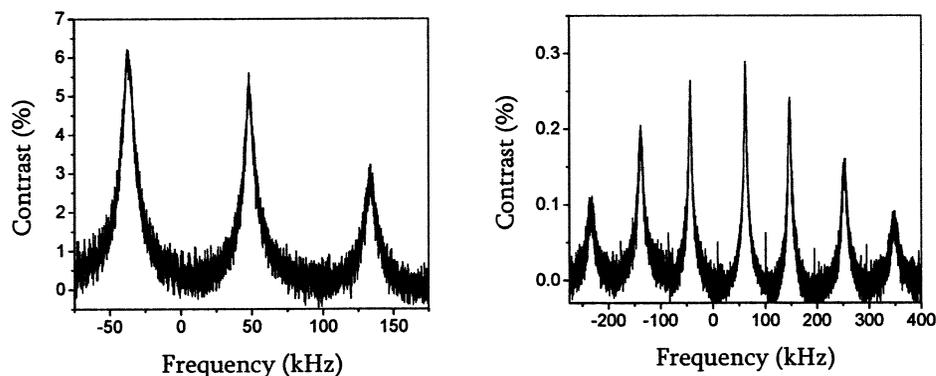
Fig. 2. CPT spectra for the two chip-scale atomic clocks for circularly polarized light in a longitudinal magnetic field. The left spectrum was taken on the D$_1$ line of ^{87}Rb, the right one on the D$_2$ line of Cs.

To explain the need for this higher Rb density, we consider a major difference between the D$_1$ and the D$_2$ line: the existence of a second, incoherent dark state for circularly polarized light on the D$_1$ line. For any alkali atom, the outermost Zeeman substate of the higher ground-state hyperfine level, the so called stretched state, does not couple to the light resonant with the D$_1$ transition. Atoms therefore accumulate in that state, contributing neither to the single-photon absorption, nor to the CPT resonance. But they can collide with other alkali atoms in the CPT state, which results in a broadening of the CPT resonance line. We suspect that this is a reason for the higher operating temperature and broader CPT linewidth.

It can be seen in Fig.2 (right) that the spectrum for the D$_2$ line of Cs is largely symmetric about the center resonance. The corresponding spectrum for the D$_1$ line of ^{87}Rb is much more asymmetric. This increased asymmetry is further evidence that optical pumping of the atoms into the non-absorbing stretched is occurring for excitation on the D$_1$ line. The depolarization cross sections of the excited states for the common buffer gases like Ne, Ar, and N$_2$ are roughly an order of magnitude bigger for the D$_2$ than for the D$_1$ line [10]. We estimate that a depolarizing collision happens roughly every 4 ns if the Rb atom is in the P$_{1/2}$ excited state and every 0.4 ns if the Cs atom is in the P$_{3/2}$ excited state. With natural lifetimes of the excited states of about 30 ns we expect no optical pumping to be present for the D$_2$ line. In the case of the Rb D$_1$ line though, pumping may be present. This can be another reason for the higher operating densities for the Rb D$_1$ CSAC.

When the device is operating as a frequency reference, the higher signal amplitude of the resonance excited using the D_1 line of ^{87}Rb leads to a fractional frequency instability of 4×10^{-11} at 1 sec of integration time, compared to $2.5 \times 10^{-10} / \tau^{1/2}$ for the D_2 line of cesium. But at the same time, the Rb cell had to be heated to 120 °C, using 160 mW of power compared to 69 mW required to heat the Cs cell to 85 °C, partly because a substantial fraction of the Rb atoms accumulate in the non-absorbing stretched state. Hence, excitation on the D1 transition appears to result in a better frequency stability, but requires more electrical power to operate.

Applications of chip-scale atomic clocks include handheld devices that range from jam-resistant GPS receivers to mobile communication and navigation systems. These systems require frequency stabilities in the 10^{-11} range over time periods longer than a few minutes, which cannot be achieved with low-power quartz crystals. Chip-scale atomic magnetometers could find uses ranging from geophysical mapping [11] to the mapping of the human heart beat [12, 13] and general magnetic sensors.

[1] S. Knappe, V. Shah, P. Schwindt, L. Hollberg, J. Kitching, L. Liew, and J. Moreland, "A microfabricated atomic clock", Appl. Phys. Lett. **85**, 1460-1462 (2004).

[2]] P. Schwindt, S. Knappe, V. Shah, L. Hollberg, J. Kitching, L. Liew, and J. Moreland, "A Chip-Scale Atomic Magnetometer," Appl. Phys. Lett., in press.

[3] J. Vig, "Military applications of high-accuracy frequency standards and clocks" **40**, 522, (1993).

[4] H. Fruehauf, 'Fast "direct-P(Y)" GPS signal acquisition using a special portable clock,' *Proc 33rd Ann. Precise Time and Time Interval (PTTI) Meeting,* 359-370 (2001).

[5] E. Arimondo, *Progress in Optics XXXV,* E. Wolf, ed., 257 (Elsevier, Amsterdam,1996).

[6] L-A. Liew, S. Knappe, J. Moreland, H. Robinson, L. Hollberg and J. Kitching, "Microfabricated alkali atom vapor cells," Appl. Phys. Lett. **84**, 2694-2696 (2004).

[7] S. Knappe, V. Velichansky, H.G. Robinson, L. Liew, J. Moreland, J. Kitching, and L. Hollberg, "Atomic Vapor Cells for Miniature Frequency References," Proc. Of the 2003 IEEE International Frequency Control Symposium and PDA Exhibition Jointly with the 17th European Frequency and Time Forum, 31-32, 2003.

[8] M. Stahler, R. Wynands, S. Knappe, J. Kitching, L. Hollberg, A. Taichenachev, and V. Yudin, "Coherent population trapping resonances in thermal Rb-85 vapor: D-1 versus D-2 line excitation," **27**, 1472-1474, (2002).

[9] R. Lutwak, D. Emmons, T. English, W. Riley, A. Duwel, M. Varghese, D.K. Serkland, G.M. Peake, "The Chip-Scale Atomic Clock - Recent Development Progress," Proc. 34th Annual Precise Time and Time Interval Systems and Applications Meeting, San Diego, CA, December 2-4, 2003.

[10] J. Vanier and C. Audoin, "The Physics at Atomic Frequency References," Bristol: Adam-Hilger, 1989

[11] T. R. Clem, "Superconducting magnetic gradiometers for underwater target detection," Naval Engineers J. **110**, 139-149 (1998).

[12] M. N. Livanov, A. N. Kozlov, S. E. Sinelnikova, J. A. Kholodov, V. P. Markin, A. M. Gorbach, A. V. Korinewsky, "Record of the human magnetocardiogram by the quantum gradiometer with optical pumping, " Adv. Cardiol. **28**, 78 (1981)

[13] G. Bison, R. Wynands, A Weis, "A laser-pumped magnetometer for the mapping of human cardiomagnetic fields, " Appl. Phys. B **76**, 325 (2003).